

A. VAŠKO*[#], J. BELAN*, E. TILLOVÁ*

STATIC AND DYNAMIC MECHANICAL PROPERTIES OF NODULAR CAST IRONS

Effects of charge composition on microstructure, mechanical and fatigue properties of nodular cast irons have been studied. For experiments, five melts of nodular cast iron were used – three types of unalloyed nodular cast irons (with different ratio of steel and pig iron in a charge and different additives for regulation of the chemical composition) and two types of alloyed nodular cast irons (SiMo- and SiCu- nodular cast iron). The microstructure of the specimens was evaluated according to a norm and by automatic image analysis. The mechanical properties were investigated by the tensile test, impact bending test and Brinell hardness test. The fatigue tests were carried out at sinusoidal cyclic push-pull loading at ambient temperature. The best mechanical properties were reached in the nodular cast iron alloyed by Si and Cu, what is related to its microstructure.

Keywords: nodular cast iron, microstructure, mechanical properties, fatigue, failure mode

1. Introduction

Nodular cast iron, also referred to as ductile cast iron or spheroidal cast iron, is a group of graphitic cast irons, which contains graphite in the form of nodules. Its mechanical properties are similar to steel, but far exceed those of standard cast irons. Due to spheroidal shape of graphite, the nodular cast iron has higher tensile strength and plasticity, as well as higher fatigue strength than other types of graphitic cast irons. Mechanical properties of nodular cast iron are strongly dependent on the microstructure (character of the matrix and the shape, size and count of graphitic nodules) which can be affected by the charge composition, chemical composition or through subsequent heat treatment. Nodular cast iron can be produced from steel scrap or pig iron. For regulation of the chemical composition, such additives as carburizer, silicon carbide or ferrosilicon can be used, and some alloying additives can also be added [1,2].

The nodular cast irons alloyed by Si and Mo are often used for high temperature applications, for example castings of the exhaust pipes of the combustion engine or turbo charger housings. The SiMo-nodular cast iron usually has a ferritic matrix, but may also contain pearlite and carbides. Increasing content of silicon promotes the stability of the microstructure and properties at low and high temperature by forming a highly ferritic matrix structure and by raising the austenite transformation temperature. Increasing concentration of silicon increases the yield strength, but lowers toughness and elongation. Therefore, the material can be very brittle at room temperature. Molybdenum partially segregates during the solidification and forms a carbidic phase on grain boundaries. This carbidic network improves the dimen-

sional stability, increases the tensile strength, creep resistance and corrosion resistance but reduces plastic properties [3-7].

The nodular cast irons alloyed by Si and Cu are used in various components of tribo-technical units. The SiCu-nodular cast iron is characterized by a high content of pearlite in a matrix and the presence of inclusions of a structurally free copper-bearing phase. Copper is a graphitizing element and it increases the degree of pearlitization of the structure. By hardening ferrite and pearlite, copper increases strength and hardness of nodular cast iron. It also rises the corrosion resistance, improves wear resistance and decreases friction coefficient of nodular cast irons [8-12].

The aim of this study is to compare the microstructure, static (tensile behavior and hardness) and dynamic (impact and fatigue strength) properties of five melts of nodular cast iron – three types of unalloyed nodular cast irons (with different charge composition) and two types of alloyed nodular cast irons described above (SiMo-nodular cast iron and SiCu-nodular cast iron).

2. Experimental material and methods

Five melts of nodular cast iron with different charge composition were used for the experiments. Melting was realised in electric induction furnaces at the Department of Technological Engineering, Faculty of Mechanical Engineering, University of Žilina, Slovak Republic and at the Department of Foundry Engineering, Faculty of Mechanical Engineering, Brno University of Technology, Czech Republic.

Previous study [13] has showed that the best mechanical properties from 10 experimental melts of unalloyed nodular cast

* UNIVERSITY OF ŽILINA, FACULTY OF MECHANICAL ENGINEERING, DEPARTMENT OF MATERIALS ENGINEERING, UNIVERZITNÁ 8215/1, 010 26 ŽILINA, SLOVAKIA

Corresponding author: alan.vasko@fstroj.uniza.sk

iron were reached in the melt made of 60% of steel and 40% of pig iron with SiC additive. It is related to the microstructure of the melt, which is characterized by the highest ratio of perfectly-nodular graphite, the smallest size of graphite and the highest count of graphitic nodules. Therefore, the same melt was chosen for next experiments (melt 1) together with the melt made of steel with SiC additive (melt 2) and the melt made of 60% of steel and 40% of pig iron with FeSi additive (melt 3). Moreover, two melts of alloyed nodular cast iron were chosen for the experiments – nodular cast iron alloyed by 4% of silicon and 1% of molybdenum, which corresponds to EN-GJS-SiMo4-1 (melt 4), and nodular cast iron alloyed by 4% of silicon and 1.5% of copper, which corresponds to EN-GJS-SiCu4-1.5 (melt 5).

Charge composition of the melts is given in Table 1. The basic charge of the melts was made up of steel, pig iron and additives for regulation of the chemical composition, i.e. carburizer, silicon carbide SiC90 and ferrosilicon FeSi75. Alloying additives, i.e. ferromolybdenum FeMo65 or copper, were added only to the charge of alloyed melts. The content of these additives was chosen to achieve required chemical composition of the melts and eutectic degree approximately $S_C \approx 1.0$ (Table 2). In all the melts, FeSiMg7 modifier was used for modification and FeSi75 inoculant was used for inoculation.

TABLE 1

Charge composition of the melts

Melt	Steel (%)	Pig iron (%)	Addition for regulation of the chemical composition	Alloying addition	Modifier & inoculant
1 (unalloyed)	60	40	carburizer + SiC90	—	FeSiMg7 + FeSi75 + cover sheet
2 (unalloyed)	100	0		—	
3 (unalloyed)	60	40	carburizer + FeSi75	—	
4 (GJS-SiMo)	60	40		FeMo65	
5 (GJS-SiCu)	60	40		Cu	

TABLE 2

Chemical composition of the melts

Melt	Content of chemical elements (weight%)								S_c
	C	Si	Mn	P	S	Cr	Mo	Cu	
1	3.58	2.43	0.39	0.05	0.03	0.08	0.01	0.01	1.01
2	3.70	2.84	0.17	0.03	0.04	0.09	0.01	0.01	1.09
3	3.61	2.23	0.23	0.05	0.03	0.07	0.01	0.01	1.01
4	3.02	4.09	0.38	0.03	0.03	0.08	0.94	0.11	1.00
5	3.28	4.16	0.36	0.03	0.04	0.07	0.01	1.39	1.09

All melts of nodular cast irons were cast into sand molds in the shape of the Y blocks (Fig. 1). Test specimens for metallographic analysis, mechanical tests and fatigue tests were machined from the Y blocks.

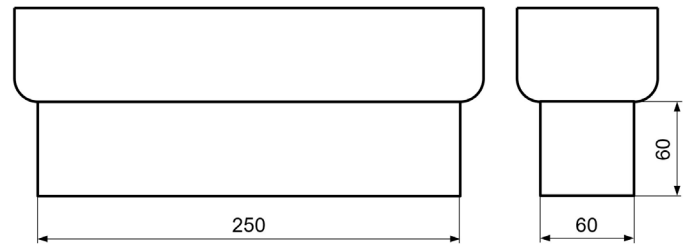


Fig. 1. Shape and dimensions of the Y block

The metallographic analysis of the specimens of nodular cast irons was done by the light metallographic microscope Neophot 32. The specimens for metallographic analysis were taken out from the Y blocks, prepared by usual metallographic procedure and etched by Nital. Microstructure of the specimens was evaluated according to STN EN ISO 945 (STN 42 0461) and by automatic image analysis [14]. The image analysis system NIS-Elements AR 4.20 was used for the evaluation of shape factor, equivalent diameter of graphite, count of graphitic nodules per unit area and content of ferrite. The final values are the average of at least 10 measurements, each at different place of the specimen.

The tensile test was performed according to STN EN ISO 6892-1 by means of the testing system Instron 5985 with a loading range $F = 0$ to 50 kN. For the tensile test, cylindrical test specimens with diameter $d_0 = 10$ mm and measured length $l_0 = 50$ mm were used. The impact bending test was executed according to STN EN ISO 148-1 by means of the Charpy hammer PSW 300 with a nominal energy of 300 J. For the impact bending test, test specimens of square cross-section with a width $a_0 = 10$ mm and length $l_0 = 55$ mm without notch were used. The Brinell hardness test was done according to STN EN ISO 6506-1 by means of the hardness tester CV-3000 LDB with a hard-metal ball of diameter $D = 10$ mm forced into specimens under the load $F = 29\,430$ N (3000 kp). The final values of mechanical properties were determined as an average of three measurements.

The low frequency fatigue tests were carried out according to STN 42 0362 by means of the fatigue experimental machine Zwick/Roell Amsler 150HFP 5100. The equipment uses the resonance principle with constant or variable amplitude and mean load [15-16]. The fatigue tests were realised at sinusoidal cyclic push-pull loading (stress ratio $R = -1$) in the high cycle fatigue region (from 10^5 to 10^7 cycles) at frequency $f \approx 120$ Hz. For the fatigue tests, specimens of circular cross-section with a diameter $d_0 = 8$ mm were used (Fig. 2). For the fatigue tests, 10 to 15 specimens from every melt of nodular cast iron were used to determine the Wöhler curve (relationship between the amplitude of stress σ_a and number of cycles to failure N_f) and the fatigue strength. For comparison, the high frequency fatigue tests at frequency $f \approx 20$ kHz were carried out using the ultrasonic fatigue testing device KAUP-ZU [17]. Both fatigue tests (low and high frequency fatigue tests) were realised at ambient temperature ($T = 20 \pm 5^\circ\text{C}$).

The microfractographic analysis was made by the scanning electron microscope VEGA II LMU on fracture surfaces of the specimens after fatigue tests [18-21].

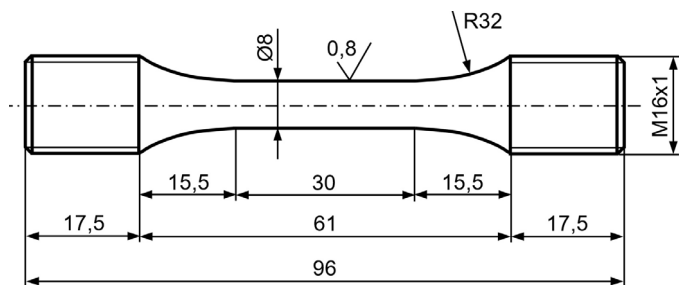


Fig. 2. Test specimen used for fatigue tests

3. Experimental results and discussion

The results of metallographic analysis are presented in Table 3. Microstructure of the specimens was evaluated according to STN EN ISO 945 (STN 42 0461) and by automatic image analysis (shape factor, equivalent diameter of graphite, count of graphitic nodules per unit area and content of ferrite).

From a microstructural point of view, the specimens from unalloyed melts are ferrite-pearlitic nodular cast irons (Fig. 3) with similar content of ferrite in the matrix, similar shape, size and count of graphitic nodules (Table 3). The highest content of ferrite was reached in the melt 2, made of steel and SiC additive

(approximately 78%), and in the melt 1, made of 60% of steel and 40% of pig iron with SiC additive (74%). Graphite occurs in perfectly-nodular and imperfectly-nodular shape in all the specimens. The highest ratio of perfectly-nodular graphite (the highest shape factor) was reached in the melt 1 (approximately 0.87). Size of graphite is from 15 to 60 μm , but in all the specimens the size within 30-60 μm predominates. The smallest size of graphite (the smallest equivalent diameter of graphite) was achieved in the melt 1 (23.5 μm). The same melt has the highest count of graphitic nodules per unit area (almost 200 mm^{-2}).

The specimen from the melt 4, alloyed by Si and Mo, is a ferrite-pearlitic nodular cast iron and the specimen from the melt 5, alloyed by Si and Cu is a pearlite-ferritic nodular cast iron (Fig. 4). Content of ferrite in the specimen of GJS-SiCu is lower than in the specimen of GJS-SiMo because of pearlitizing effect of copper. Graphite occurs predominantly in perfectly-nodular shape in both specimens. Size of graphite in the specimen of GJS-SiCu is smaller than in the specimen of GJS-SiMo, but an average count of graphitic nodules per unit area in the specimen of GJS-SiCu is higher than in the specimen of GJS-SiMo. Different content of ferrite in the matrix as well as different size of graphite and count of graphitic nodules in the individual specimens is caused by different charge composition.

TABLE 3

Microstructure of examined nodular cast irons

Melt	Microstructure (according to STN EN ISO 945)	Shape factor*	Equivalent diameter of graphite (μm)	Count of graphitic nodules (mm^{-2})	Content of ferrite (%)
1	80%VI6/7 + 20%V6 – Fe94	0.87	23.5	199.8	74.0
2	70%VI6/7 + 30%V6 – Fe94	0.82	24.4	179.8	78.0
3	70%VI6 + 30%V6 – Fe80	0.79	28.4	151.0	65.2
4	80%VI6 + 20%V6 – Fe55	0.88	31.2	122.8	59.4
5	80%VI6/7 + 20%V6 – Fe15	0.84	24.3	172.4	19.7

* $S = 4\pi A/P^2$ (A – area of a graphitic nodule, P – perimeter of a graphitic nodule)

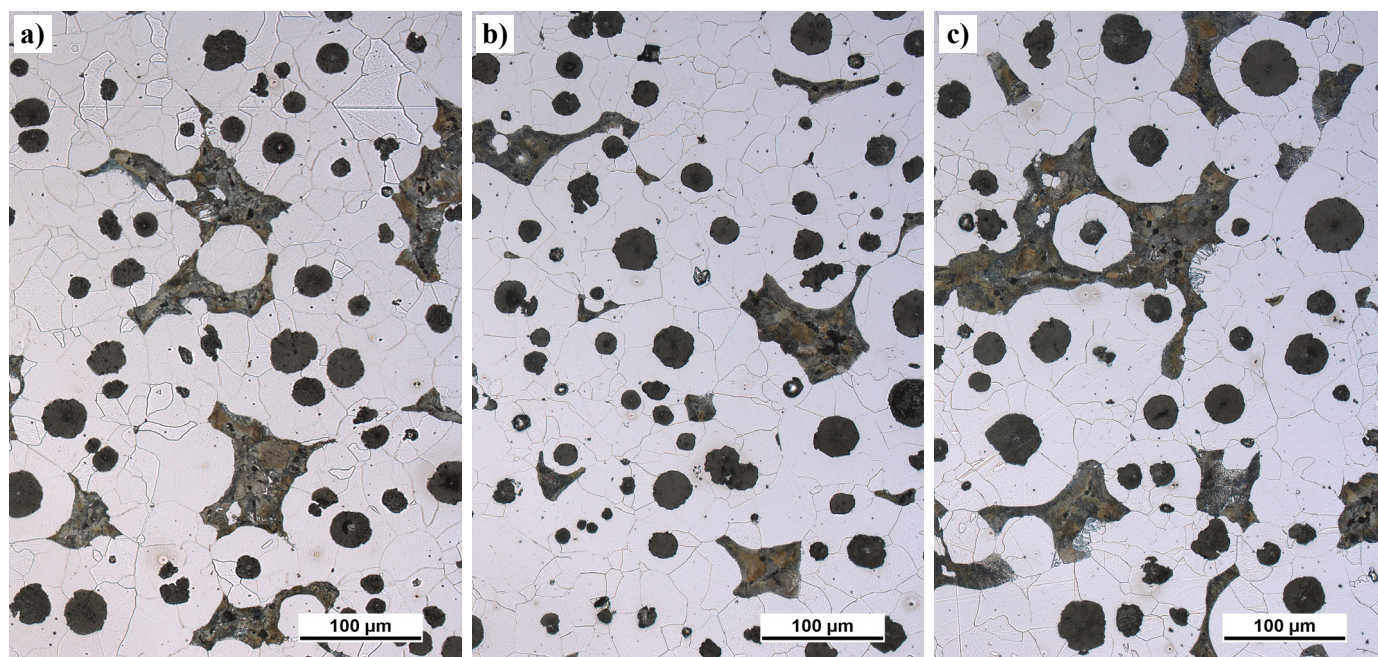


Fig. 3. Microstructure of unalloyed nodular cast irons, etched by 1% Nital, a) melt 1, b) melt 2, c) melt 3

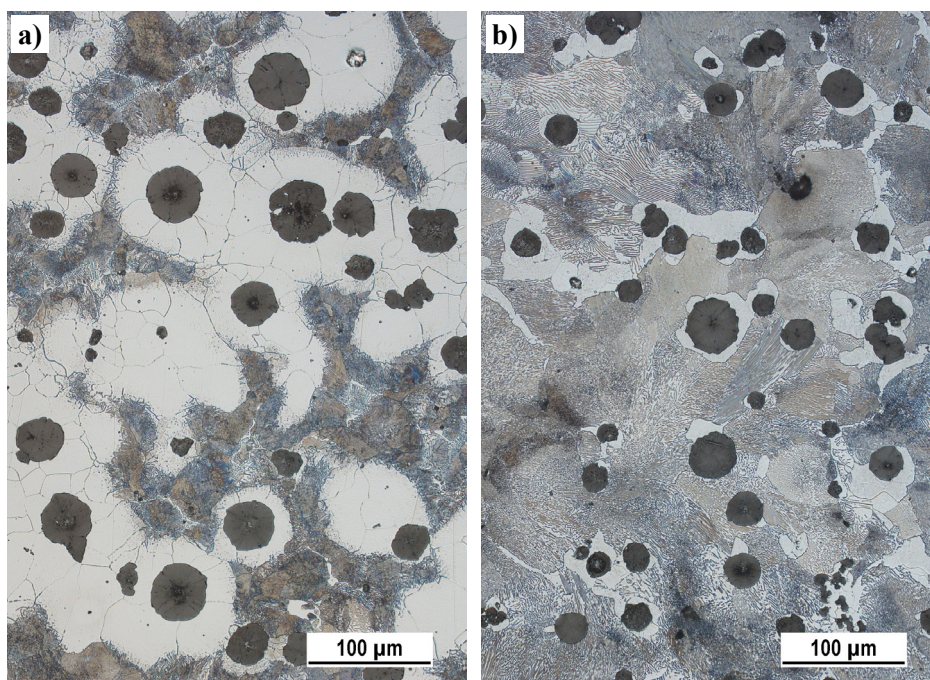


Fig. 4. Microstructure of alloyed nodular cast irons, etched by 1% Nital, a) melt 4 (GJS-SiMo), b) melt 5 (GJS-SiCu)

The results of mechanical tests (tensile strength R_m , elongation A , absorbed energy K and Brinell hardness HBW) are given in Table 4. The best mechanical properties from the unalloyed melts were reached in the melt 1, made of 60% of steel and 40% of pig iron with SiC additive, which has the highest ratio of perfectly-nodular graphite, the smallest size of graphite and the highest count of graphitic nodules. The specimens from alloyed melts have better tensile strength and hardness but worse plasticity. The specimen of GJS-SiCu has higher tensile strength and Brinell hardness, but lower elongation and absorbed energy than the specimen of GJS-SiMo. That is related to the microstructure of the specimens, especially to the character of matrix (content of ferrite and pearlite) and also to the size of graphite and count of graphitic nodules.

The results of fatigue tests (relationship between stress amplitude σ_a and number of cycles to failure N_f) for unalloyed nodular cast irons are shown in Fig. 5. Wöhler curves were obtained at low frequency cyclic loading ($f \approx 120$ Hz) (Fig. 5a)

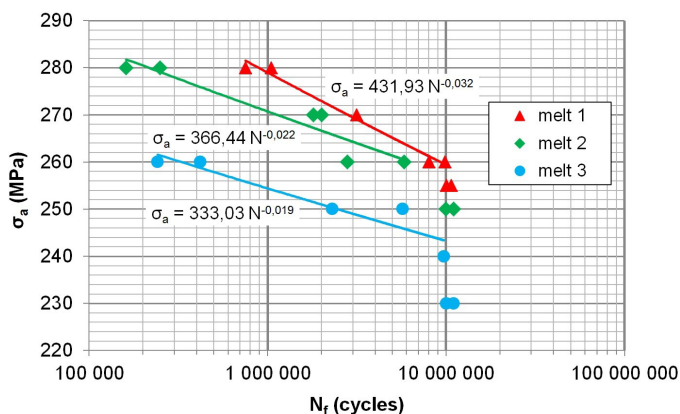


Fig. 5. Wöhler curves $\sigma_a = f(N)$ of unalloyed nodular cast irons, a) low frequency cyclic loading ($f \approx 120$ Hz), b) high frequency cyclic loading ($f \approx 20$ kHz)

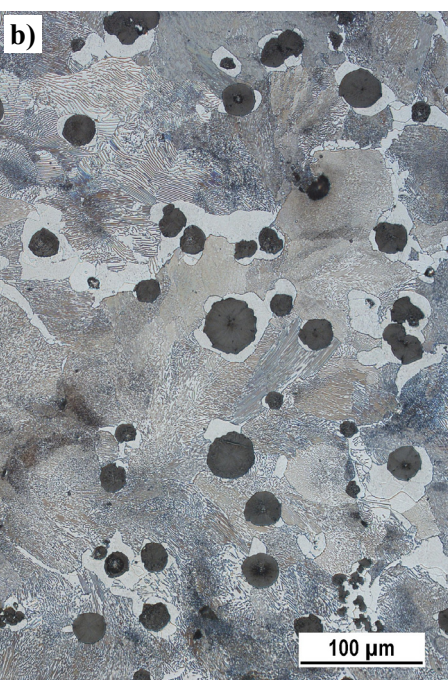


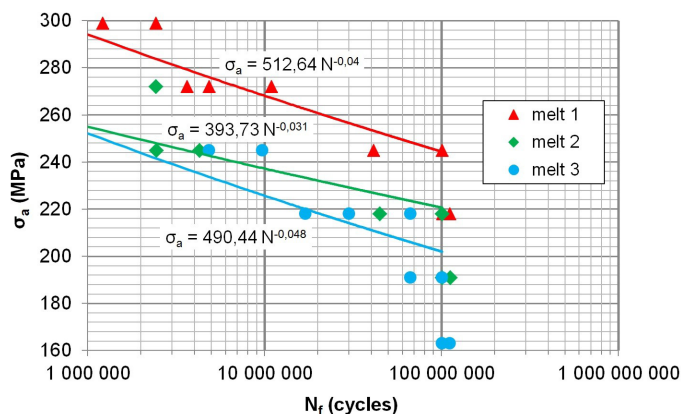
TABLE 4

Mechanical properties of examined nodular cast irons

Melt	R_m (MPa)	A (%)	K (J)	HBW 10/3000
1	539.0	4.0	30.6	198.3
2	515.7	3.7	17.2	192.7
3	462.6	2.7	24.0	192.5
4	573.9	1.4	11.3	213.7
5	652.7	0.7	8.0	247.3

and high frequency cyclic loading ($f \approx 20$ kHz) (Fig. 5b). In both cases, the number of cycles to failure increases with a decreasing stress amplitude. The results obtained at high frequency cyclic loading are in a good agreement with the results obtained at low frequency cyclic loading [22].

The results of fatigue tests for alloyed nodular cast irons are shown in Fig. 6. Wöhler curves were obtained only at low frequency cyclic loading ($f \approx 75$ Hz). The number of cycles to failure also increases with a decreasing stress amplitude.



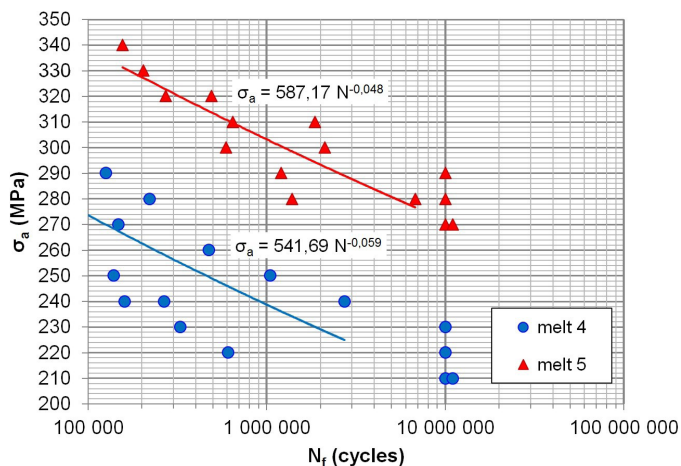


Fig. 6. Wöhler curves $\sigma_a = f(N)$ of alloyed nodular cast irons; low frequency cyclic loading ($f \approx 75$ Hz)

The values of fatigue strength σ_c determined for $N = 10^7$ cycles (at low frequency cyclic loading) and for $N = 10^8$ cycles (at high frequency cyclic loading) in comparison with tensile strength R_m are given in Table 5. In both cases, the fatigue strength in unalloyed melts increases with an increasing tensile

TABLE 5

Comparison of tensile strength R_m and fatigue strength σ_c

Cyclic loading		Low frequency	High frequency
Melt	R_m (MPa)	σ_c (MPa) for $N = 10^7$ cycles	σ_c (MPa) for $N = 10^8$ cycles
1	539.0	255	218
2	515.7	250	191
3	462.6	230	163
4	573.9	210	
5	652.7	270	

strength. The highest fatigue strength from the unalloyed melts was reached in the melt 1, made of 60% of steel and 40% of pig iron with SiC additive, which also has the best mechanical properties. The melt 5, alloyed by Si and Cu, has higher fatigue strength than unalloyed melts but the melt 4, alloyed by Si and Mo, has lower fatigue strength. That is related to the charge composition of melts and microstructure of the specimens. Better fatigue properties of the melt GJS-SiMo in comparison with the other melts would become evident at higher temperatures.

The fatigue fracture surfaces of analysed specimens from unalloyed melts (Fig. 7) do not show any remarkable differences;

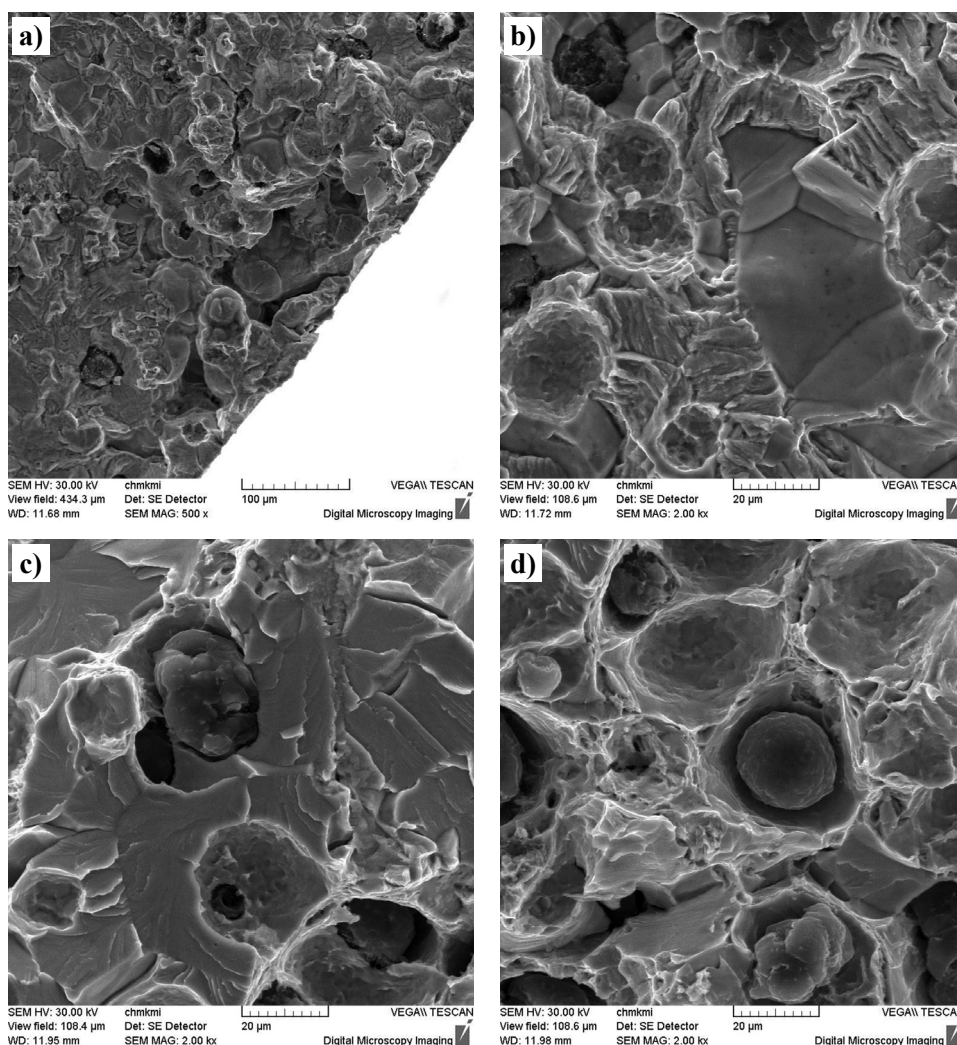


Fig. 7. Fatigue fracture surfaces of the specimens of unalloyed nodular cast irons, SEM, a) initiation zone of fatigue failure, b) trans- and inter-crystalline fatigue failure, c) transcrystalline cleavage, d) transcrystalline ductile failure

they are characteristic of mixed mode of fracture. On the fracture surface, it is possible to distinguish the area of propagation of fatigue crack from the area of final rupture. The fatigue fracture was initiated by a cavity (casting defect) that acted as a primary notch (Fig. 7a). The fatigue fracture is characteristic of intercrystalline fatigue failure of ferrite around graphitic nodules and transcrystalline fatigue failure of ferrite and pearlite in the rest of area (Fig. 7b). The final rupture is characteristic of transcrystalline cleavage of ferrite and pearlite with river drawing on facets (Fig. 7c) and transcrystalline ductile failure of ferrite with dimple morphology (Fig. 7d). No significant differences were observed by the comparison of fracture surfaces of the specimens from unalloyed and alloyed melts. The fatigue failure of the specimens from alloyed melts has also a mixed character of fracture; intercrystalline fatigue failure predominates near graphitic nodules and transcrystalline fatigue failure predominates in the rest of area. These failure micromechanisms are in agreement with the microstructure of the material.

4. Conclusions

The experimental results can be summarized to the following points:

- The charge composition (ratio of steel and pig iron, kind of additives for regulation of the chemical composition and alloying additives) influences the microstructure and consequently, mechanical and fatigue properties of nodular cast iron are changed;
- The best mechanical properties from the unalloyed melts were achieved in the melt 1, made of 60% of steel and 40% of pig iron with SiC additive, which has the highest shape factor, the smallest size of graphite and the highest count of graphitic nodules;
- The specimens from alloyed melts have better tensile strength and hardness but worse plasticity than unalloyed melts. The melt 5, alloyed by Si and Cu, has the highest tensile strength, hardness and fatigue strength, but the lowest plasticity, that is related to pearlitizing effect of copper. Positive effect of molybdenum on fatigue properties would be evident at higher temperatures;
- Fatigue failure micromechanisms of the nodular cast irons correspond to their microstructure. They depend especially on the content of ferrite in the matrix and its purity, which has a connection with the charge composition; higher ratio of transcrystalline ductile failure is characteristic for higher content of ferrite in the matrix.

Acknowledgement

The research has been supported by the Scientific Grant Agency of Ministry of Education, Science, Research and Sport of Slovak Republic, grant project

VEGA No. 1/0398/19 and by the Culture and Educational Grant Agency of Ministry of Education, Science, Research and Sport of Slovak Republic, grant project KEGA No. 049ŽU-4/2017.

REFERENCES

- [1] O. Bokůvka, G. Nicoletto, M. Guagliano, L. Kunz, P. Palček, F. Nový, M. Chalupová, *Fatigue of Materials at Low and High Frequency Loading*, EDIS, Žilina (2014).
- [2] R. Konečná, G. Nicoletto, L. Bubenko, S. Fintová, *Engineering Fracture Mechanics* **108**, 251-262 (2013).
- [3] J. Roučka, E. Abramová, V. Kaňa, *Archives of Metallurgy and Materials* **63** (2), 601-607 (2018).
- [4] M. Stawarz, *Archives of Foundry Engineering* **17** (1), 147-152 (2017).
- [5] V. Norman, P. Skoglund, D. Leidermark, J. Moverare, *International Journal of Fatigue* **99** (2), 258-265 (2017).
- [6] P. Matteis, G. Scavino, A. Castello, D. Firrao, *Procedia Materials Science* (3), 2154-2159 (2014).
- [7] L.M. Åberg, C. Hartung, *Transactions of the Indian Institute of Metals* **65** (6), 633-636 (2012).
- [8] G. Gumienny, B. Kacprzyk, J. Gawroński, *Archives of Foundry Engineering* **17** (1), 51-56 (2017).
- [9] E. Konca, K. Tur, E. Koc, *Metals* **7** (8), 320-328 (2017).
- [10] A.A. Razumakov, N.V. Stepanova, I.A. Bataev, O.G. Lenivtseva, I.I. Riapolova, K.I. Emurlaev, *Materials Science and Engineering* **124**, 012136 (2016).
- [11] J. Lacaze, J. Sertucha, *International Journal of Cast Metals Research* **29** (1-2), 73-77 (2016).
- [12] G.I. Silman, V.V. Kamynin, V.V. Goncharov, *Metal Science and Heat Treatment* **49** (7-8), 387-393 (2007).
- [13] A. Vaško, *Materials Science (Medžiagotyra)* **14** (4), 311-314 (2008).
- [14] P. Skočovský, A. Vaško, *Quantitative Evaluation of Structure of Cast Irons (in Slovak)*, EDIS, Žilina (2007).
- [15] M. Uhrčík, P. Palček, M. Chalupová, M. Frkáň, *MATEC Web of Conferences* **157**, 07013 (2018).
- [16] P. Kopas, L. Jakubovičová, M. Vaško, M. Handrik, *Procedia Engineering* **136**, 193-197 (2015).
- [17] L. Trško, F. Nový, O. Bokůvka, M. Jambor, *Journal of Visualized Experiments* **133**, e57007 (2018).
- [18] G. Hütter, L. Zybelle, M. Kuna, *Engineering Fracture Mechanics* **147**, 388-397 (2015).
- [19] X. Wu, G. Quan, R. Macneil, Z. Zhang, C. Sloss, *Metallurgical and Materials Transactions A* **45A** (11), 5085-5097 (2014).
- [20] A. Ghahremaninezhad, K. Ravi-Chandar, *Acta Materialia* **60** (5), 2359-2368 (2012).
- [21] R. Gurbuz, A. Kalkanli, H. Gonenc, *Canadian Metallurgical Quarterly* **43** (1), 137-144 (2004).
- [22] A. Vaško, *Archives of Metallurgy and Materials* **62** (4), 2205-2210 (2017).